Kinetic model for a step edge in epitaxial growth

Russel E. Caflisch,[1] Weinan E,[2] Mark F. Gyure,[3] Barry Merriman,[1] and Christian Ratsch[1,3]
[1]*Department of Mathematics, University of California at Los Angeles, Los Angeles, California 90095-1555*
[2]*Courant Institute of Mathematical Sciences, New York University, New York, New York 10012*
[3]*HRL Laboratories, LLC, 3011 Malibu Canyon Road, Malibu, California 90265*
(Received 12 January 1999)

A kinetic theory is formulated for the velocity of a step edge in epitaxial growth. The formulation involves kinetic, mean-field equations for the density of kinks and ''edge adatoms'' along the step edge. Equilibrium and kinetic steady states, corresponding to zero and nonzero deposition flux, respectively, are derived for a periodic sequence of step edges. The theoretical results are compared to results from kinetic Monte Carlo (KMC) simulations of a simple solid-on-solid model, and excellent agreement is obtained. This theory provides a starting point for modeling the growth of two-dimensional islands in molecular-beam epitaxy through motion of their boundaries, as an alternative to KMC simulations. [S1063-651X(99)02806-8]

PACS number(s): 81.15.Aa, 81.15.Hi, 81.15.Kk

I. INTRODUCTION

Modeling epitaxial growth is extremely challenging due to the wide range of length and time scales represented by problems of practical interest. In spite of the dramatic increase in available computational power and improved numerical algorithms over the past decade, the only viable approach remains construction of a hierarchy of models, each of which is valid over a much narrower range. For example, *ab initio* methods are capable of describing atomistic processes in great detail, but are completely inappropriate for describing growth on macroscopic length and time scales. Similarly, kinetic atomistic models for epitaxial growth (such as simple solid-on-solid models) have had success describing growth processes on length scales of several thousand angstroms, but still fall short of being able to describe growth on the scales of interest for device applications. As understanding of the relevant physics on each scale improves, the burden begins to fall more heavily on bridging these length and time scales, i.e., developing methodologies for transferring information from models at smaller scales to parameters in models that describe larger scales.

In this paper, we lay a foundation for one approach to connecting the atomistic and continuum scales in epitaxial growth. Specifically, we develop a theory for the velocity of a step edge whose direct inputs are kinetic rates from atomistic processes. We expect this theory to be applicable not only for determining the macroscopic velocity of a step edge, but also the velocity of the boundary of a two-dimensional island in layer-by-layer molecular-beam epitaxy (MBE) growth. This velocity could then be used in either a simulation of step dynamics or, alternatively, in an ''island dynamics'' simulation of epitaxial growth such as that described in [1], and therefore could provide a bridge between microscopic and macroscopic length and time scales.

The velocity of a step edge in crystal growth was determined in the classic paper of Burton, Cabrera, and Frank (BCF) [2] for a system with small supersaturation. Modifications of the BCF theory to include deviations from equilibrium have been proposed earlier in [3–6], but these all rely fundamentally on the system being close to equilibrium. For thin-film growth by MBE, the supersaturation is typically quite large since there is almost no desorption. Hence the growth is controlled by kinetic, rather than equilibrium, considerations, and an appropriate continuum model should reflect this.

The main purpose of this paper is to describe a macroscopic theory for epitaxial growth and, in particular, determine the velocity of a step edge based strictly on kinetics with no near-equilibrium assumptions. The theory reduces to that of [2] when the system is in equilibrium. This theory is formulated in terms of the density of kinks and ''edge adatoms'' on the step edge, as illustrated in Fig. 1. Edge adatoms are defined to be those atoms which are bound to a step edge, but still have mobility along the step. The density of kinks and edge adatoms is determined using a mean-field theory for their interactions. Our analysis starts from the kinetic exchange rates (phrased in terms of ''diffusion coefficients'' and ''coordination numbers'') for atoms on the surface. These parameters specify details of the dynamics of epitaxial growth at a microscopic level, and are used here as the microscopic information that is needed for the macroscopic model.

In some cases these rates can be obtained from experimental data, although their determination is often indirect and generally requires application of a theory whose basic assumptions may not always be valid. For example, the diffusion coefficient of adatoms on a surface can be determined indirectly by measuring the density of islands in submonolayer deposition experiments and applying basic nucleation theory [7,8]. This assumes, of course, that basic nucleation

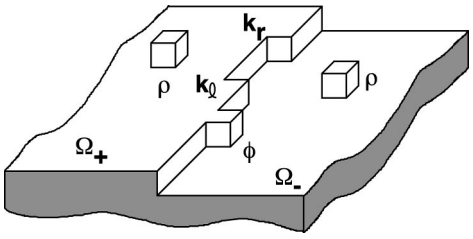

FIG. 1. Schematic drawing of an epitaxial surface, showing a step edge, adatoms, kinks, and edge adatoms.

theory is valid for the material system and parameter ranges of interest, which is not always the case. These kinetic rates can also, in principle, be directly determined from *ab initio* computations [9]. This is a promising approach and although such calculations are computationally demanding, this method is more likely to produce reliable numbers since no indrect interpretation of experimental data is required.

Although our kinetic, mean-field approach to epitaxial growth seems quite natural, we know of only one reference in which something similar is proposed. In [10], Voronkov derived a related theory for the velocity of a step on a crystal surface that is far from equilibrium. Rather than starting from microscopic exchange rates, his analysis depends on the ''effective supersaturation'' at the step, which is difficult to obtain directly. His results include a formula for step edge velocity in terms of effective supersaturation, but he does not provide a full model for the evolution of the epitaxial surface, as we formulate below. In addition, he assumed that the attachment to the step is directly from the vapor above the epitaxial surface, whereas we have included the adatom density on the terraces adjacent to the step.

This paper is organized as follows. The epitaxial growth model is derived in Secs. II and III. The former section contains only equations derived from macroscopic arguments, while all of the relations that depend on the kinetic mean-field approximation are reserved for the latter section. The model is phrased in terms of a general set of diffusion coefficients and coordination numbers. Detailed balance implies certain relations among the diffusion coefficients, as described in Sec. IV. In Sec. V, we determine specific parameters which correspond to those in an atomistic solid-on-solid (SOS) model. Equilibrium solutions are derived in Sec. VI and kinetic steady-state solutions are derived in Sec. VII. KMC results presented in these sections confirm the validity of this theory for the SOS model. Since the equilibrium solutions are consistent with those of BCF, the predicted differences between equilibrium and the kinetic steady-state solutions show the significance of the kinetic effects; this is discussed in Sec. VIII, along with the application of this theory to a continuum description of epitaxial growth.

II. MODEL OF THE STEP EDGE: MACROSCOPIC EQUATIONS

In epitaxial growth, adatoms are deposited on a terrace and diffuse until they attach to a step edge or collide with another adatom. The adatom diffusion equation is

$$\partial_t \rho - D_T \nabla^2 \rho = -\tau^{-1}\rho + F - M \tag{2.1}$$

in which ρ is the adatom density, D_T is the adatom diffusion coefficient on a terrace, F is the deposition flux rate, M is the loss due to nucleation, and τ^{-1} is the desorption rate, which will be omitted in the subsequent discussion.

We define f_+ to be the net flux of adatoms to the step edge from the upper terrace, and f_- the net flux from the lower terrace. In terms of $f_\pm$, the boundary conditions for the diffusion equation are

$$v\rho_+ + D_T \boldsymbol{n}\cdot\boldsymbol{\nabla}\rho_+ = -f_+, \tag{2.2}$$

$$v\rho_- + D_T \boldsymbol{n}\cdot\boldsymbol{\nabla}\rho_- = f_-, \tag{2.3}$$

in which ρ_+ and ρ_- are the limiting values of ρ at the edge from the upper terrace and the lower terrace, respectively, $\boldsymbol{n}$ is the normal pointing into the lower terrace, and v is the normal velocity of the boundary in the direction $\boldsymbol{n}$. The term $v\rho_\pm$ on the left is due to the motion of the boundary and would not be present if the boundary were not moving. Although this term is typically quite small in epitaxial growth, without it mass is not exactly conserved.

Edge adatoms diffuse along a step edge until they attach to a kink site, at which point we consider them to be part of the step. The diffusion equation for the edge-adatom density φ is

$$\partial_t \varphi - D_E \partial_s^2 \varphi = f_+ + f_- - f_0 \tag{2.4}$$

in which D_E is the edge diffusion coefficient, s is the arc-length variable along the edge, and f_0 is the net flux of edge adatoms to kinks. In Eq. (2.4), the flux terms $f_\pm$ serve as sources of edge adatoms as described in the next section.

As a step edge moves by atoms attaching to a kink, the kink moves along the edge. Since the step edges are one dimensional, there are two kinds of kinks (cf. Fig. 1): those that move to the left, which we call left-facing kinks with density $k_\swarrow$, and those that move to the right, which we call right-facing kinks with density k_r. We denote the total density of kinks as $k = k_r + k_\swarrow$. For simplicity we assume the atomistic hopping rates (i.e., the diffusion coefficients described below) are the same for left- and right-facing kinks. In particular, this implies that the macroscopic speed is the same for left- and right-facing kinks, so that the velocities are $-w$ and w for left- and right-facing kinks, respectively. The resulting convective flux of kinks with respect to arc length s is $w(k_r - k_\swarrow)$. In addition, as described in the next section, there are two processes for the net gain or loss of kink pairs; the net gain in kink pairs due to ''nucleation/breakup'' is denoted by g and the net loss in kink pairs due to ''creation/annihilation'' is denoted by h. Note that g and h include both gain and loss terms. In the kinetic steady state that is of most interest for MBE growth, there is a net gain from nucleation/breakup and a net loss from creation/annihilation, which is the reason for taking $g > 0$ to correspond to net gain and $h > 0$ to correspond to net loss. Therefore, the kink density k evolves according to the convective equation

$$\partial_t k + \partial_s [w(k_r - k_\swarrow)] = 2(g - h). \tag{2.5}$$

Additional relations between the kink densities k, k_r, and $k_\swarrow$ are implied by the geometry of the step edge. Consider a crystal with lattice constant a, and a step edge that is nearly parallel to one of the primitive (i.e., lowest index) crystallographic directions. Let $\boldsymbol{e}_0$ be the corresponding crystallographic axis, and $\boldsymbol{n}$ the unit normal to the macroscopically curved step edge. Let θ denote the angle between $\boldsymbol{e}_0$ and $\boldsymbol{n}$. Along the step edge, the densities of right- and left-facing kinks satisfy

$$k_r + k_\swarrow = k, \tag{2.6}$$

$$k_r - k_\ell = -a^{-1}\tan\theta. \tag{2.7}$$

The flux f_0 of edge adatoms to kinks can be determined by macroscopic considerations, as follows: Denote the step edge as Γ, separating the upper terrace Ω_+ from the lower terrace Ω_-. Neglect deposition flux F and desorption for the moment, since they are spatially distributed and do not affect the form of f_0. As mentioned above, we do not consider edge adatoms to be part of the step edge. Conservation of mass then says that any loss of adatoms on the terraces must be due to either growth of the step edge or accumulation of edge adatoms; i.e.,

$$-\frac{d}{dt}\int_{\Omega_+\cup\Omega_-}\rho dA = a^{-2}\int_\Gamma v\,ds + \frac{d}{dt}\int_\Gamma \varphi ds. \tag{2.8}$$

On the other hand, the only way for adatoms to leave the terraces is through the fluxes $f_\pm$, so that

$$\frac{d}{dt}\int_{\Omega_+\cup\Omega_-}\rho dA = -\int_\Gamma (f_+ + f_-)ds. \tag{2.9}$$

In addition, the rate of change of arc length of a moving curve is equal to the product of the normal velocity v and the curvature κ, from which it follows that

$$\frac{d}{dt}\int_\Gamma \varphi ds = \int_\Gamma \varphi_t + \varphi\kappa v\,ds. \tag{2.10}$$

Combining these, we obtain

$$\begin{aligned} -a^{-2}\int_\Gamma v\,ds &= \frac{d}{dt}\int_{\Omega_+\cup\Omega_-}\rho dA + \frac{d}{dt}\int_\Gamma \varphi ds \\ &= -\int_\Gamma (f_+ + f_-)ds + \int_\Gamma (\varphi_t + \varphi\kappa v)ds \\ &= \int_\Gamma (-f_0 + \varphi\kappa v)ds. \end{aligned} \tag{2.11}$$

By properly restricting the integral to a short segment of the boundary Γ, this identity implies that the integrands $-a^{-2}v$ and $-f_0+\varphi\kappa v$ in the first and last integrals must be the same, which shows that the flux rate for edge adatoms to kinks is

$$f_0 = v(\varphi\kappa + a^{-2}). \tag{2.12}$$

Finally, as derived in [4], the normal velocity v for a step edge must satisfy

$$v = awk\cos\theta \tag{2.13}$$

since the velocity of the edge is due to the growth of the upper terrace by motion of the kinks.

To summarize, the adatom density satisfies the diffusion equation (2.1) with boundary conditions (2.2) and (2.3). The equations for edge-adatom density φ and kink density k are Eqs. (2.4) and (2.5). Constitutive laws for these equations include the macroscopic conditions (2.6) and (2.7) for k_r and k_l, as well as Eq. (2.12) for f_0. The velocity v for the step edge is determined by the Eq. (2.13). All of these equations are macroscopic. Additional constitutive equations for M, $f_\pm$, w, g, and h will be determined in the next section.

III. MODEL OF THE STEP EDGE: MEAN-FIELD INTERACTION TERMS

In the preceding section, macroscopic analysis was used to derive equations for the adatom, edge adatom, and kink densities. Here we formulate expressions for M, $f_\pm$, w, g, and h in terms of diffusion coefficients and geometric constants, which we will refer to as ''coordination numbers.''

Consider an interaction process P involving transitions from state A to state B. Let c_P be the ''coordination number'' which counts the number of paths through which this transition can occur. Although transition from A to B through different paths may occur at different rates (and even involve several different atomistic processes), we may form a single effective rate α_{AB} for all transitions from A and B. It is convenient to replace the transition rate by an effective ''diffusion coefficient,'' which is defined as $D_{AB}=a^2\alpha_{AB}$ in which a is the lattice constant. Although the diffusion coefficient D_{BA} may differ from D_{AB}, the coordination numbers for the process and its inverse must be the same; hence the notation c_P.

We will use diffusion coefficients (D_{AB}) rather than transition rates (α_{AB}) in the remainder of this paper since the most significant transitions involve the motion of atoms along terraces and step edges which result in diffusion of adatoms and edge adatoms. The transition rates might be more natural for some of the other processes, but can also be misleading since some of them may involve several atomistic processes each with their own rate. So in order to emphasize the generality of our model and achieve notational uniformity, we use effective diffusion coefficients, defined as above to have the correct units of $(\text{length})^2/\text{time}$.

If the probability for occurrence of a state A is denoted as $p(A)$, then the total rate for transitions from A to B is $c_P(D_{AB}a^{-2})p(A)$. Most of the significant processes involve interactions between two or more adatoms, edge adatoms, or kinks, so that $p(A)$ should be a two (or more) particle probability density function. The mean-field assumption is that this density can be approximated by a product of single-particle density functions. This approximation should be valid if the particle densities are small and there is some mixing in the system. This is the main assumption in our model and its accuracy will be tested by comparison of results from our theory to those from kinetic Monte Carlo simulations.

First consider the rate of island nucleation. Assuming that the critical cluster size for adatoms on a terrace is one (i.e., clusters of size two or larger are stable islands), then the loss term M due to island nucleation is

$$M = 2c_M D_T a^2 \rho^2. \tag{3.1}$$

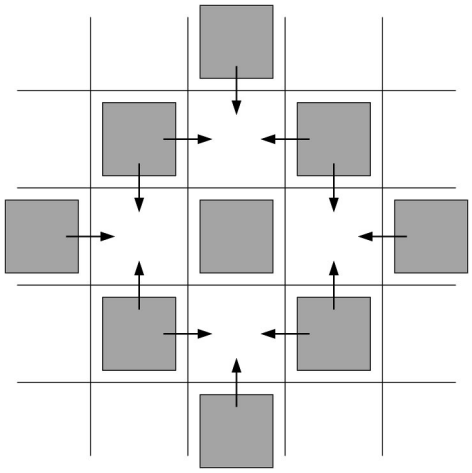

FIG. 2. Illustration of the nucleation process. For a fixed adatom (center), this shows the $c_M = 12$ ways that a second adatom can attach to nucleate a new island.

The coordination number c_M measures the number of ways that two adatoms can hop together to form a cluster at a given location as shown in Fig. 2. For the general model formulated here, this figure (as well as Figs. 3, 4, and 5) is only a caricature of the processes, but for the cubic SOS model developed later, this figure correctly describes these processes. The corresponding inverse process, the breakup of small clusters, is ignored. Note that the term ρ^2 is justified through the mean-field approximation.

Next consider the fluxes $f_\pm$, which result from an exchange of atoms between the terraces and an edge. They are written in terms of diffusion coefficients and coordination numbers as

$$f_+ = c_{f+}(D_{TE}^+ a\rho_+ - D_{ET}^+ \varphi)a^{-2}, \tag{3.2}$$

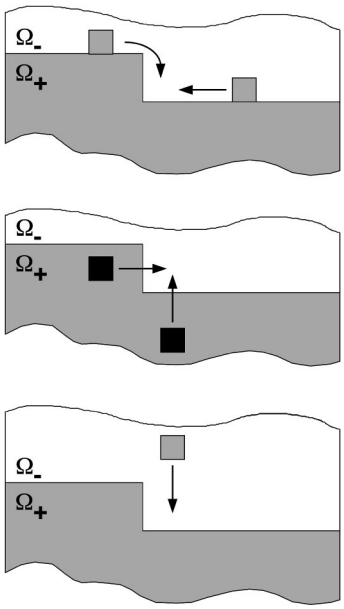

FIG. 3. Illustration of the kink velocity w. This shows the number of ways that an adatom can hop to a fixed kink site: $c_{w1} = 2$ for an edge adatom (top); $c_{w2} = 2$ for an adatom from the upper terrace (middle); $c_{w3} = 1$ for an adatom from the lower terrace (bottom).

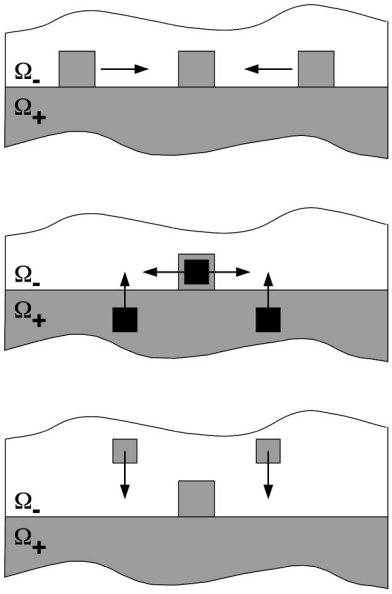

FIG. 4. Illustration of the rate g for nucleation/breakup of kink pairs. This shows the number of ways that an atom can hop to a fixed edge adatom: $c_{g1} = 2$ for an edge adatom (top); $c_{g2} = 4$ for an adatom from the upper terrace (middle); $c_{g3} = 2$ for an adatom from the lower terrace (bottom).

$$f_- = c_{f-}(D_{TE}^- a\rho_- - D_{ET}^- \varphi)a^{-2}. \tag{3.3}$$

In these equations, D_{TE}^+ is the diffusion coefficient for the transition from the upper terrace (T) to an edge (E), and D_{ET}^+ is the diffusion coefficient for the inverse transition from edge to terrace. The coordination number for transitions between the edge and the upper terrace is c_{f+}. Transitions to

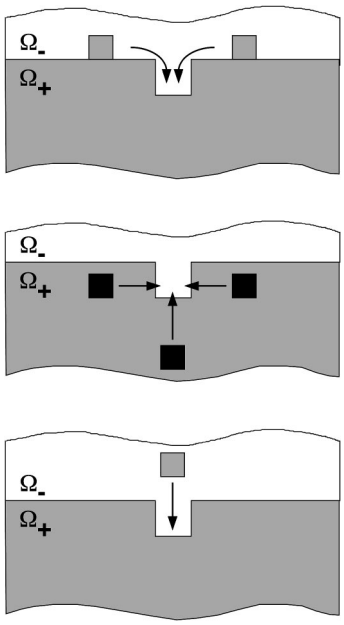

FIG. 5. Illustration of the rate h for creation/annihilation of kink pairs. This shows the number of ways that an adatom can fill in an empty site between two kinks: $c_{h1} = 2$ for an edge adatom (top); $c_{h2} = 3$ for an adatom from the upper terrace (middle); $c_{h3} = 1$ for an adatom from the lower terrace (bottom).

and from the lower terrace have diffusion coefficients D_{TE}^{-} and D_{ET}^{-}, and coordination number c_{f-}.

The kink velocity w is determined by three processes: transitions between an edge (E) and a kink (K), transitions between the upper terrace (T^{+}) and a kink (K), and transitions between the lower terrace (T^{-}) and a kink (K). The rates for these three processes are denoted by w_1, w_2, and w_3, respectively, formulas for which are derived next. The three processes are illustrated in the upper, middle, and lower diagrams of Fig. 3.

First consider transitions between edge adatoms and a given kink. The attachment rate is $c_{w1}D_{EK}\varphi a^{-1}$ in which $a\varphi$ is the probability for an edge adatom to be at a particular site adjacent to the kink, the coordination number c_{w1} counts the number of relevant adjacent sites, and $D_{EK}a^{-2}$ is the transition rate to go from an adjacent site to the kink. The detachment rate is $c_{w1}D_{KE}a^{-2}$. Note that since this calculation is performed with reference to a given kink, as is appropriate for a calculation of velocity, there is no factor of k.

The attachment rate for adatoms from the upper terrace to a given kink is $c_{w2}D_{TK}^{+}\rho_{+}$ in which $a^2\rho_{+}$ is the probability for an adatom to be at a particular site on the upper terrace adjacent to the kink, the coordination number c_{w2} counts the number of relevant adjacent sites, and $D_{TK}^{+}a^{-2}$ is the transition rate to go from an adjacent site to the kink. The detachment rate is $c_{w2}D_{KT}^{+}a^{-2}$.

Similarly, the attachment and detachment rates for an adatom from the lower terrace to the kink are $c_{w3}D_{TK}^{-}\rho_{-}$ and $c_{w3}D_{KT}^{-}a^{-2}$, respectively.

We combine these three processes to get the kink velocity w, which is a times the net rate of attachment and detachment. The result is

$$w = w_1 + w_2 + w_3 \tag{3.4}$$

in which

$$\begin{aligned} w_1 &= c_{w1}(D_{EK}\varphi - D_{KE}a^{-1}), \\ w_2 &= c_{w2}(D_{TK}^{+}a\rho_{+} - D_{KT}^{+}a^{-1}), \\ w_3 &= c_{w3}(D_{TK}^{-}a\rho_{-} - D_{KT}^{-}a^{-1}). \end{aligned} \tag{3.5}$$

Next, consider the gain and loss of kinks. This occurs in two ways: In the first process, which we call nucleation/breakup, a left-right kink pair (facing away from each other and consisting of two atoms) can nucleate by two atoms coming together along the edge, and it can break up by an atom moving away. The net gain of kinks due to nucleation/breakup is denoted $2g$, in which g is the net rate of gain of kink pairs. In the second process, which we call creation/annihilation, a right-left kink pair (facing toward each other and separated by a single atomic vacancy along the edge) can form due to detachment of a single atom from a straight edge, and the kink pair can be destroyed by an atom filling in the vacant spot. The net loss of kink pairs due to creation/annihilation is denoted $2h$, in which h is the net rate of loss of kink pairs. The signs are chosen so that g and h are positive in epitaxial growth. These processes involve transitions between the adatoms on the upper and lower terraces (T^{+} and T^{-}), edge adatoms (E), atoms at a kink (K), and atoms in the bulk (B) by which we mean those that are in a straight step edge.

First consider g: Nucleation of a kink pair occurs by an atom moving next to an existing edge adatom. The moving atom can be either an edge adatom or an adatom from the upper or lower terrace. The net gain rates for these processes are denoted g_1,g_2, and g_3, respectively. They are illustrated in the upper, middle and lower diagrams in Fig. 4, respectively.

The nucleation rate due to collision of two edge adatoms is $c_{g1}D_{EK}\varphi^2 a^{-1}$ in which φ is the density of edge adatoms, $a\varphi$ is the probability of an edge adatom in a site adjacent to the first edge adatom, c_{g1} is the number of such sites, and $a^{-2}D_{EK}$ is the hopping rate. Breakup of a kink pair, resulting in two edge adatoms, occurs at rate $c_{g1}D_{KE}k_r k_{\diagup} a^{-1}$, in which $ak_r k_{\diagup}$ is the density of kink pairs, c_{g1} counts the number of ways that they can break up into two edge adatoms, and $a^{-2}D_{KE}$ is the hopping rate for this transition.

We combine these expressions with similar expressions for nucleation and breakup involving an edge adatom and an adatom to obtain

$$g = g_1 + g_2 + g_3 \tag{3.6}$$

in which

$$\begin{aligned} g_1 &= c_{g1}(D_{EK}\varphi^2 - D_{KE}k_r k_{\diagup})a^{-1}, \\ g_2 &= c_{g2}(D_{TK}^{+}a\rho_{+}\varphi - D_{KT}^{+}k_r k_{\diagup})a^{-1}, \\ g_3 &= c_{g3}(D_{TK}^{-}a\rho_{-}\varphi - D_{KT}^{-}k_r k_{\diagup})a^{-1}. \end{aligned} \tag{3.7}$$

Finally, consider h which is the net rate of annihilation of kink pairs due to two processes: The first process is the annihilation of a kink pair which faces each other and is separated by a single site. The kink pair is annihilated and the step edge is completed by an adatom moving into the gap between the kinks. The second, inverse process is the creation of a kink pair by removal of a single atom from a straight edge. The atom that fills in the gap or is removed from the straight edge can be either an edge adatom, or an adatom from the upper or lower terrace. These three processes are denoted by h_1, h_2, and h_3, respectively, and they are illustrated in the upper, middle, and lower diagrams in Fig. 5, respectively.

Suppose that the atom that moves is an edge adatom. Then the annihilation rate is $c_{h1}D_{EB}\varphi k_r k_{\diagup}$, in which $ak_r k_{\diagup}$ is the density of kink pairs facing toward each other and separated by a single site, $a\varphi$ is the probability of an edge adatom in a given site adjacent to the kink pair, c_{h1} counts the number of such sites, and $D_{EB}a^{-2}$ is the hopping rate for the edge adatom. The rate of creation of kink pairs is $c_{h1}D_{BE}a^{-3}$ in which a^{-1} is the density of sites from which an atom can detach (this neglects the presence of edge adatoms and kinks, which is a higher-order correction), c_{h1} counts the number of ways that an atom can detach to form an edge adatom, and $D_{BE}a^{-2}$ is the hopping rate from the bulk to the edge.

We combine these expressions with the corresponding expressions for attachment and detachment of adatoms to obtain

$$h = h_1 + h_2 + h_3 \tag{3.8}$$

in which

$$\begin{aligned} h_1 &= c_{h1}(D_{EB}\varphi k_r k_{/\!/} - D_{BE}a^{-3}), \\ h_2 &= c_{h2}(D_{TB}^{+}a\rho_{+}k_r k_{/\!/} - D_{BT}^{+}a^{-3}), \\ h_3 &= c_{h3}(D_{TB}^{-}a\rho_{-}k_r k_{/\!/} - D_{BT}^{-}a^{-3}). \end{aligned} \tag{3.9}$$

To summarize, we have derived in this section expressions for the kink velocity w, the fluxes f_+ and f_-, and the creation and loss terms M, g, and h.

IV. EQUILIBRIUM AND DETAILED BALANCE

Before finishing the derivation of the epitaxial growth model, we need to consider the consistency conditions required for detailed balance. Here we derive the equilibrium values of adatom, edge adatom, and kink densities and then obtain the consistency conditions on the diffusion coefficients.

At equilibrium, detailed balance implies that f_+, f_- and each of the three terms in g, h, and w must vanish. In addition, ρ is constant in equilibrium, so that $\rho_+ = \rho_-$ and assuming that the step edge is parallel to a fundamental crystal direction implies that $k_r = k_{/\!/} = k/2$. The equations $g_1 = g_2 = g_3 = 0$ and $w_1 = 0$ imply $w_2 = w_3 = 0$. Of the remaining nine equations, three provide equations for ρ, φ, and k, and six are consistency conditions for the diffusion coefficients.

From the w_1, g_1, and f_+ equations, we obtain the following equations for ρ, φ, and k in equilibrium:

$$\rho = (D_{ET}^{+}/D_{TE}^{+})(D_{KE}/D_{EK})a^{-2}, \tag{4.1}$$

$$\varphi = (a/4)k^2, \tag{4.2}$$

$$k = 2(D_{KE}/D_{EK})^{1/2}a^{-1}. \tag{4.3}$$

The equations for g_2, h_1, h_2 then imply

$$(D_{TK}^{+}/D_{KT}^{+})(D_{ET}^{+}/D_{TE}^{+})(D_{KE}/D_{EK}) = 1, \tag{4.4}$$

$$(D_{EB}/D_{BE})(D_{KE}/D_{EK})^2 = 1, \tag{4.5}$$

$$(D_{TB}^{+}/D_{BT}^{+})(D_{ET}^{+}/D_{TE}^{+})(D_{KE}/D_{EK})^2 = 1. \tag{4.6}$$

The remaining equations for f_-, g_3, and h_3 then imply

$$(D_{ET}^{-}/D_{TE}^{-}) = (D_{ET}^{+}/D_{TE}^{+}) \tag{4.7}$$

$$(D_{KT}^{-}/D_{TK}^{-}) = (D_{KT}^{+}/D_{TK}^{+}) \tag{4.8}$$

$$(D_{BT}^{-}/D_{TB}^{-}) = (D_{BT}^{+}/D_{TB}^{+}). \tag{4.9}$$

This concludes the derivation of the mean-field kinetic model for epitaxial growth. Equations (2.1)–(2.7), (2.12), (2.13), and (3.1)–(3.9) define the model in general form. Equations (4.4)–(4.9) are detailed balance conditions that restrict the possible values of the diffusion coefficients. In deriving these consistency conditions, we have also derived the equilibrium solutions, Eqs. (4.1)–(4.3), for this model.

V. THE CUBIC SOLID-ON-SOLID MODEL

In the previous sections, we formulated a general model for epitaxial growth, involving diffusion coefficients and coordination numbers. Now we determine these parameters for an atomistic cubic solid-on-solid (SOS) model and use them in our continuum model which we will now refer to as the continuum SOS model. We then make specific predictions for the behavior of this model. The cubic SOS model we use is nearly identical to the model described in [11,12]. While not intended to describe any specific material system, this model nevertheless contains all the basic mechanisms present in epitaxial growth of many real materials. This model has two parameters, E_S and E_N, which describe the energy barrier for adatom hopping on a terrace and the additional barrier for hopping with a single nearest neighbor. The total barrier E_b for hopping is then given by $E_b = E_S + nE_N$, where n is the total number of in-plane nearest neighbors [11,12].

The dynamics of this model involve the following four diffusion coefficients (which, for this simple model, are hopping rates multiplied by a^2): D_T is the diffusion coefficient for an adatom on a terrace, D_E is the diffusion coefficient for an edge adatom along an edge, D_K is the diffusion coefficient for an atom from a kink, and D_B is the diffusion coefficient for an atom from a straight edge. These are given by

$$\begin{aligned} &D_T = a^2\nu e^{-E_S/k_BT}, \quad D_E = D_T e^{-E_N/k_BT}, \\ &D_K = D_T e^{-2E_N/k_BT} = D_E^2/D_T, \\ &D_B = D_T e^{-3E_N/k_BT} = D_E^3/D_T^2, \end{aligned} \tag{5.1}$$

in which ν is an attempt frequency, typically of order 10^{13} sec^{-1}, T is temperature, and k_B is the Boltzmann factor.

In terms of these diffusion coefficients, the diffusion coefficients for individual transitions are

$$\begin{aligned} &D_{TE}^{\pm} = D_{TK}^{\pm} = D_{TB}^{\pm} = D_T, \quad D_{ET}^{\pm} = D_{EK} = D_{EB} = D_E, \\ &D_{KT}^{\pm} = D_{KE} = D_{KB} = D_K, \quad D_{BT}^{\pm} = D_{BE} = D_{BK} = D_B. \end{aligned} \tag{5.2}$$

All hops are assumed to be to a nearest-neighbor site with one exception: at a kink, an atom can hop between the kink and its diagonal neighbor along the edge. Diagonal hops were included because they allow atoms to hop around corners and across kinks, resulting in compact islands in kinetic

Monte Carlo simulations of this model. Step-edge asymmetry, with different hopping rates from the upper and lower terraces to the edge, could easily be included but is omitted here for simplicity.

Next we determine the coordination numbers for this model. First consider nucleation in which one adatom hops to a neighboring site of another adatom. To avoid duplication in counting, pick a site for the atom that does not hop and count the ways in which an atom hops to it. As illustrated in Fig. 2, there are two possible routes from each of the four diagonal sites and one possible route from each of the four sites that are next nearest neighbors in the horizontal or vertical directions. Therefore $c_M=12$.

Next consider the kink velocity w. To be specific, consider a right-facing kink. As shown in Fig. 3, there are two sites from which an edge adatom can hop to the kink, one to the right of the kink and one directly attached to the kink (the latter joins the kink by a diagonal hop), so that $c_{w1}=2$. From the lower terrace, there is only a single position, diagonally opposite the corner of the kink, from which an adatom can hop to the kink, so that $c_{w3}=1$. Finally, from the upper terrace, an adatom can hop to the kink either from the left (on top of the end of the kink) or from below (opposite the site to the right of the kink), so that $c_{w2}=2$. Together these show that

$$w=2D_E\varphi+D_Ta(2\rho_++\rho_-)-5D_Ka^{-1}. \tag{5.3}$$

Next consider the nucleation and breakup of kink pairs, which are described by the term g and illustrated in Fig. 4. For a given edge adatom, there are two ways (from the right or from the left) in which a second edge adatom can hop to it, so that $c_{g1}=2$. From the lower terrace, there are also two ways (from the right or left) in which an adatom can hop to it, so that $c_{g3}=2$. Finally, from the upper terrace, there are four ways (one from each of the sites to the right or left and two ways from directly on top of the edge adatom), so that $c_{g2}=4$. It then follows that

$$g=2\varphi[a^{-1}D_E\varphi+aD_T(2\rho_++\rho_-)]-8a^{-1}D_Kk_rk_\diagup. \tag{5.4}$$

Similarly, as shown in Fig. 5, $c_{h1}=2$, $c_{h2}=3$, and $c_{h3}=1$ so that

$$h=[2D_E\varphi+aD_T(3\rho_++\rho_-)]k_rk_\diagup-6D_Ba^{-3}. \tag{5.5}$$

VI. THERMODYNAMIC EQUILIBRIUM

Using the specific diffusion coefficients and coordination numbers for the continuum SOS model from the preceding section, we now formulate predictions from the model in two particular regimes: equilibrium and kinetic steady states. The analytic results from the model are directly compared to the results of KMC simulations to provide validation for the model and, in particular, the mean-field approximation.

Equilibrium values for the adatom, edge adatom, and kink densities were derived in Sec. IV. Here we specialize those results to the continuum SOS model described in the preceding section. The detailed balance results (4.1)–(4.3) together with the specification of the diffusion coefficients (5.2) result in the following formulas:

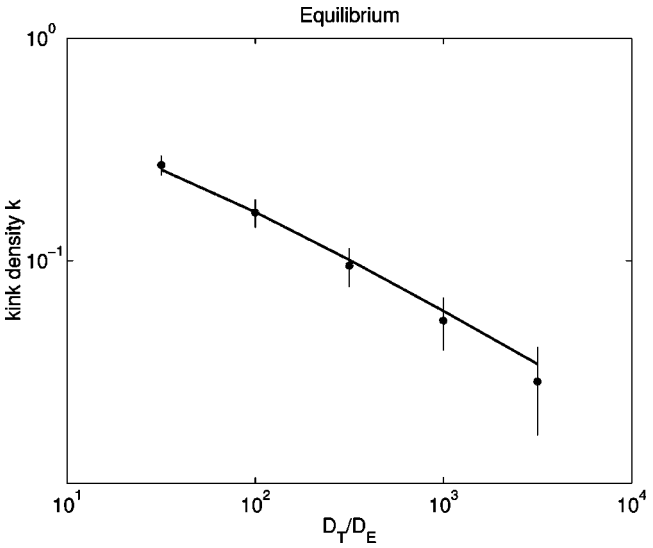

FIG. 6. Kink density k vs time t for equilibrium with $F=0$ as determined from KMC computations (•, with error bars) and BCF theory (solid line).

$$\rho=(D_E/D_T)a^{-1}\varphi, \tag{6.1}$$

$$\varphi=(a/4)k^2, \tag{6.2}$$

$$k=2(D_K/D_E)^{1/2}a^{-1}. \tag{6.3}$$

The detailed balance requirements (4.4) and (4.7)–(4.9) follow directly from Eq. (5.2) for the diffusion coefficients. The two remaining conditions (4.5) and (4.6) are then equivalent to the detailed balance requirement that

$$D_K^2=D_ED_B, \tag{6.4}$$

which is a direct consequence of Eqs. (5.1).

The three equations (6.1)–(6.3) are consistent with the equilibrium density values derived in Appendix A of [2], except that [2] includes the effects of kinks of size larger than one, resulting in

$$k=2\sqrt{D_K/D_E}(1+\sqrt{D_K/D_E})^{-1}a^{-1}. \tag{6.5}$$

This is the same as k in Eq. (6.3) in the limit of small values of D_K/D_E.

For partial validation of this step edge model, we have performed computations for the motion of a periodic series of step-edges, using standard kinetic Monte Carlo techniques to simulate the atomistic (SOS) model. Computations were performed for a range of values of diffusion coefficients (D_T,D_E) (or equivalently, binding energies E_S and E_N) and terrace widths L. Since the kink density is significantly larger than the adatom and edge-adatom densities, we use it to compare with the prediction of Eq. (6.3) or Eq. (6.5).

Figure 6 shows a comparison of the simulation results and the prediction of Eq. (6.5) for the equilibrium kink density

with $F=0$, $D_T=10^{12}$, and the ratio D_E/D_T varying between $10^{1.5}$ and $10^{3.5}$. The agreement is excellent, with the differences between theory and simulation well within one standard deviation of the simulation results. Agreement with the leading-order formula (6.3) is also good, but not quite as close as that for Eq. (6.5). These results demonstrate the accuracy of the growth model in the equilibrium regime. In particular, they confirm that our model is consistent with BCF theory for equilibria with small kink densities. This is also a first test of the validity of the mean-field approximations used in the model.

VII. KINETIC STEADY STATE FOR STEP FLOW

Finally consider a kinetic steady state consisting of a periodic sequence of steps, separated by distance L and moving at velocity v along one fundamental crystallographic direction. For nonzero deposition flux F, we find a kinetic steady state, in which $\rho=\rho(x-vt)$, φ and k are constants, and $\theta=0$.

In steady state (and neglecting desorption and nucleation), the flux to the boundaries must equal the total deposition flux, which implies

$$v=a^2(f_+ + f_-)=a^2LF. \tag{7.1}$$

The remaining steady-state equations are

$$0=f_+ + f_- - f_0, \quad 0=g-h. \tag{7.2}$$

Here we neglect the slowest processes D_K and D_B and assume that $ak \ll 1$. For the model formulated in Sec. V, one can show that $\rho_+=\rho_-$. Then the adatom, edge adatom, and kink densities are

$$\rho=(D_E/D_T)a^{-1}\varphi, \tag{7.3}$$

$$\varphi=(16a/3)k^2, \tag{7.4}$$

$$k=(\tfrac{16}{15}P_{\text{edge}})^{1/3}a^{-1}. \tag{7.5}$$

In the equation for k, P_{edge} is the edge Peclet number, defined as

$$P_{\text{edge}}=(a^3LF)/D_E, \tag{7.6}$$

which is the ratio of the total flux $f=LF$ to an edge from deposition and the diffusive flux $a^{-3}D_E$ along the edge. The exponent 1/3 in Eq. (7.5) is related to the critical size for formation of a left-right kink pair. If the critical size were j (i.e., if $j+1$ edge adatoms were required to form a stable kink pair), then the exponent would be $j/(j+2)$.

Figure 7 shows a comparison of the theoretical and computational results for kink density k for $F=1$. In this figure, the value of D_T is 10^{12}, while D_E varies between 10^4 and 10^7. The figure shows excellent agreement between the predictions of the present theory and the results of the kinetic

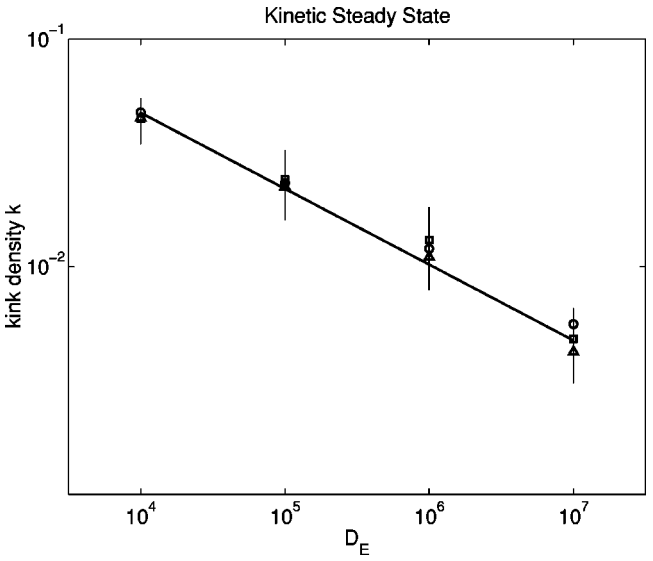

FIG. 7. Kink density k, normalized by $L^{1/3}$, vs edge diffusion coefficient D_E for kinetic steady state, for various values of terrace width L. Parameter values are flux $F=1$ and adatom diffusion $D_T=10^{12}$. Results are shown from the kinetic theory (solid line) and KMC computations with $L=25$ (squares), $L=50$ (○), and $L=100$ (△).

Monte Carlo simulation, with differences that are less than one standard deviation of the KMC results. Validation of the present theory shows the validity of the mean-field approximation, which was the main step in its derivation.

Equation (7.5) is our main result, showing the difference between the kinetic steady-state kink density and the equilibrium kink density (6.3). In deriving this result, we have ignored detachment from kinks (D_K) and from straight edges (D_B) since these are insignificant in a typical MBE growth. In equilibrium, on the other hand, detailed balance requires that each process and its inverse process must balance. As the deposition flux F is decreased, the growth is slower so that D_K and D_B can become significant. Equation (7.5) remains valid until F is so small that the value of Eq. (7.5) becomes as small as that of Eq. (6.3). This shows the connection between the equilibrium and kinetic steady-state results and that the present theory is capable of describing the transition between them.

VIII. CONCLUSIONS

The theory developed above determines the velocity of a step edge in epitaxial growth, as well as the density of edge adatoms and kinks along the edge with no near-equilibrium assumptions. The difference between the kink density in equilibrium versus kinetic steady state shows the significance of the kinetic considerations. As shown above, a virtue of the present theory is that it is valid in both the equilibrium limit and the kinetic steady-state regime. Therefore, it can be used to describe epitaxial growth for systems that are near as well as far from equilibrium. Thus it should prove to be a powerful model for investigating a wide range of epitaxial phenomena.

The model developed above is also quite general, since the macroscopic mechanisms should apply to almost any kind of epitaxial growth. Details of the specific kinetic

mechanisms at the atomistic scale are inserted into the macroscopic model through the diffusion coefficients D and coordination numbers c.

As described above, this theory involves the angle θ with one of the principal crystallographic axes $\boldsymbol{e}_0$, and therefore is restricted to boundaries that are nearly perpendicular to the fundamental crystallographic directions. Extension to an arbitrary boundary curve is effected by defining θ to be the angle with the closest crystal direction. This is probably not valid for angles near $\pi/4$, i.e., at the corners of a growing island. On the other hand, we expect that the details of the dynamics at corners are not too significant; as in a kinetic Wulff shape [13], the corners grow so fast that their motion is limited (i.e., determined) only by the dynamics away from corners. For this reason, we believe that this theory should be applicable to the motion of island boundaries during layer-by-layer MBE growth, where kinetic considerations are known to be important. We believe that this model is an important first step in bridging the atomistic and continuum length scales in epitaxial growth and will ultimately allow for simulations of continuum models that include realistic kinetic effects.

ACKNOWLEDGMENTS

We thank Richard Ross for his careful reading of the manuscript. This research was supported in part by the NSF and DARPA through Grant No. NSF-DMS9615854 as part of the Virtual Integrated Prototyping (VIP) Initiative.

[1] R. Caflisch *et al.*, Appl. Math. Lett. **12**, 13 (1999); M.F. Gyure *et al.*, Phys. Rev. E **58**, 6927 (1998).
[2] W. Burton, N. Cabrera, and F. Frank, Philos. Trans. R. Soc. London, Ser. A **243**, 299 (1951).
[3] R. Ghez, H. Cohen, and J. Keller, J. Appl. Phys. **73**, 3685 (1993).
[4] R. Ghez and S. Iyer, IBM J. Res. Dev. **32**, 804 (1988).
[5] J. Keller, H. Cohen, and G. Merchant, J. Appl. Phys. **73**, 3694 (1993).
[6] F. Liu and H. Metiu, Phys. Rev. E **49**, 2601 (1997).
[7] Y. Mo, J. Kleiner, M. Webb, and M. Lagally, Phys. Rev. Lett. **66**, 1998 (1991).
[8] H. Brune, H. Roder, C. Boragno, and K. Kern, Phys. Rev. Lett. **73**, 1955 (1994).
[9] P. Ruggerone, C. Ratsch, and M. Scheffler, in *The Chemical Physics of Solid Surfaces Vol. 8*, edited by D. King and D. Woodruff (Elsevier Science, Amsterdam, 1997), pp. 490–544.
[10] V. Voronkov, Kristallografiya **15**, 13 (1970) [Sov. Phys. Crystallogr. **15**, 8 (1970)].
[11] S. Clarke and D. Vvedensky, J. Appl. Phys. **63**, 2272 (1988).
[12] T. Shitara *et al.*, Phys. Rev. B **46**, 6815 (1992); **46**, 6825 (1992).
[13] S.J. Osher and B. Merriman, Asian J. Math. **1**, 560 (1997).